CHAPTER VI

RESULTS AND DISCUSION:

$(1-x-y)Bi_{0.5}Na_{0.5}TiO_3–xBi_{0.5}K_{0.5}TiO_3–yK_{0.5}Na_{0.5}NbO_3$

In this chapter, the results are presented for the investigation of $(1-x-y)Bi_{0.5}Na_{0.5}TiO_3–xBi_{0.5}K_{0.5}TiO_3–yK_{0.5}Na_{0.5}NbO_3$ (BNNKT) powders and ceramics using combustion technique. There are three parts, (1) the influence of firing temperature on crystal structure and microstructure of BNNKT ceramics, (2) effects of x and y on crystal structure and microstructure of BNNKT ceramics, (3) effects of x and y on electrical properties of BNNKT ceramics. The scope of electrical properties measurement include dielectric, piezoelectric ferroelectric hysteresis loop (P-E) and strain loop (S-E).

Introduction

Sensors and actuator piezoelectric ceramics are widely used in applications. These piezoelectric ceramics are mostly based on PZT ceramics, which contain more than 60% lead. Lead is varying toxic substance and environmental problem due to its high vapor pressure during sintering process. Therefore, it is very urgent to develop lead-free piezoelectric ceramics with excellent properties to replace PZT based ceramic. $Bi_{0.5}Na_{0.5}\ TiO_3$ (BNT) is considered to be a promising candidate for lead free piezoelectric ceramics because of its large remnant polarization (38 $\mu C/cm^2$) and high Curie temperature (T_c = 320 °C). However, when compared to PZT ceramics, BNT ceramics possess lower piezoelectric properties and present poling difficultly because of their high coercive field (E_c= 73 kV/cm) [58, 70, 93, 94, 95, 96]. For developing higher piezoelectric properties, binary and ternary solid solutions based on BNT were developed and shown to have electromechanical high performance at the MPB. $Bi_{0.5}Na_{0.5}\ TiO_3$-$Bi_{0.5}K_{0.5}\ TiO_3$ (BNT-BKT) binary system between rhombohedral and tetragonal phase at $0.16 \leq x \leq 0.20$, whith highest d_{33}~ 157 pC/N for x = 0.20 [1]. Kounga et al. [104] reported a small addition amount of KNN to BNT exhibited the largest polarization at x=0.03, though not yet comparable to PZT. Ternary system

of BNT-BKT-KNN based on BNT exhibited the high electrical properties in the MPB composition. These systems showed relaxor ferroelectric nature undergoing a field-induced phase transition from the relaxor state (ergodic or nonergodic) to a long-range ordered state [105]. This means polar nano-regions (PNRs) are urged to grow into micro-sized domains depending on the concentration of BKT and KNN content when electric fields is applied. As a results, coexistence of polar and non-polar phase at MPB were indicated by pinched P-E loop and large strain of ~0.48% was obtained in $0.99(0.8Bi_{0.5}Na_{0.5}TiO_3\text{-}0.2Bi_{0.5}K_{0.5}TiO_3)\text{-}0.01(0.97K_{0.5}Na_{0.5}NbO_3\text{-}0.03Bi_{0.5}K_{0.5}TiO_3)$ system with S_{max}/E_{max} 600 pm/V, which is profitable for the actuator application [106].

$(1\text{-}x\text{-}y)Bi_{0.5}Na_{0.5}TiO_3\text{–}xBi_{0.5}K_{0.5}TiO_3\text{–}yK_{0.5}Na_{0.5}NbO_3$(BNNKT) has been synthesised by using conventional solid-state method. The pure phase of KNN and BNT-BKT powders were obtained by calcination at 880 °C and 850 °C for 4 h, respectively and sintering temperatures at 1140-1170 °C for 2-4 h. it is general knowledge that the conventional solid state method required compulsory grinding different oxide mixtures for a long period of time and sintering suffers as well. The synthesized component distributions are not homogeneous and particle sizes are larger. Recently, our previous work has successfully fabricated high quality different oxide ceramics which was used as a new technology for materials synthesis such as $(Ba_{1\text{-}x}Sr_x)(Zr_xTi_{1\text{-}x})O_3$ [20], $0.79Bi_{0.5}Na_{0.5}TiO_3\text{-}0.18Bi_{0.5}K_{0.5}TiO_3\text{-}0.03BiFeO_3$ [97] $(Pb_{1\text{-}x}Ba_xTiO_3)$ [22]. This method offers several distinct advantages, like the homogeneous mixing of several components at atomic level, a simple preparation process, low firing temperature and a short dwell time. Furthermore, from a survey of the literature, BNNKT powders and ceramics prepared by the combustion method have not been studied. To understand the nature of these large strains, further studies of the relationship between phase diagrams and electrical properties are necessary by using combustion method. So, in this work, $(1\text{-}x\text{-}y)Bi_{0.5}Na_{0.5}TiO_3\text{–}xBi_{0.5}K_{0.5}TiO_3\text{–}yK_{0.5}Na_{0.5}NbO_3$($0.18\leq x\leq 0.28$ and $0\leq y\leq 0.07$) powders and ceramics were prepared by the combustion method. The optimum firing temperatures and effect of x and y contents on microstructure, phase transformation, electrical properties (dielectric, piezoelectric, P-E and S-E loops) were studied.

Experimental

(1-x-y)$Bi_{0.5}Na_{0.5}TiO_3$-x$Bi_{0.5}K_{0.5}TiO_3$-y$K_{0.5}Na_{0.5}NbO_3$ceramics (0.18≤x≤0.28, fixed y=0.03 and 0≤y≤0.07, fixed x=0.20) (abbreviated as BNNKT x/0.03 and BNNKT y/0.18) were prepared by the combustion technique.Bi_2O_3 (99.5%), Na_2CO_3 (99.5%), K_2CO_3 (98.0%), TiO_2 (99.5%) and Nb_2O_5 (> 99.95%) were chosen as the starting raw materials. For each composition, the oxides and carbonates were weighed according to the stoichiometric formula and ball milled again for 24 h. Raw materials were mixed together with fuel (glycine) in an agate mortarby use of a 2:1 ratio. The calcined powders were calcined between 600 and 850 °C for 2 h. and then ball milled again for 24 h. The calcined powders were mixed with polyvinyl alcohol and pressed into discs with a diameter of 15 mm under 150 MPa. Sintering was carried out between 1000 °C and 1050 °C for 2 h.

Phase structure of the ceramics was identified using X-ray diffraction (XRD). The grain morphology of the samples was observed by means of scanning electron microscopy (SEM). The theoretical density for each composition was calculated using the law of mixting and the densities of $Bi_{0.5}Na_{0.5}TiO_3$, $Bi_{0.5}K_{0.5}TiO_3$ and $K_{0.5}Na_{0.5}NbO_3$ pure phases, which were 5.99 g/cm^3 (JCPDS file no. 36-0340), 5.93 g/cm^3 (JCPDS file no. 36-0339) and ~4.50 g/cm^3[107], respectively. For electrical characterization, samples were polished and painted with silver paste on the surfaces. Dielectric constant and loss of the ceramics for a wide variety of frequencies in the temperature range of 50 to 450 °C were measured using LCR meter (Agilent 4284A). The polarization-electric field (P-E) hysteresis loops and strain-electric field (S-E) hysteresis loops were measured using the ferroelectric test system.

Results and Discussion

The influence of firing temperatures on crystal structure and microstructure of BNNKT ceramics

The XRD patterns of BNNKT-0.20/0.03 powders with various calcination temperatures between 600 °C and 850 °C for 2 h are shown in Figure 58. The crystal structure belonged to rhombohedral matched with JCPDS file number 360340. At temperature < 750 °C, an impurity phase of $K_4Ti_3O_8$ was discovered

(Figure 58(a)).The pure perovskite phase was found at the calcination temperature ≥ 750 °C, as shown in Figure 58.The percent perovskite phase of BNNKT can be calculated by the following equation (14). When I_{perov} and $I_{K_4Ti_3O_8}$ are the intensity of the (110) perovskite and the intensity of the highest $K_4Ti_3O_8$ peak. The percent of the perovskitephase of BNNKT-0.20/0.03 powders at various calcination temperatures wascalculated and is listed in Table 16.The percent perovskite phase in all samples increased with an increase of the calcination temperaturesand the highest percentage was observed in powders calcinedabove 750 °C.

$$\%\, Perovskite\ phase = \left(\frac{I_{Perov}}{I_{Perov} + I_{K_4Ti_3O_8}} \right) \times 100 \qquad (14)$$

Figure 59 shows the XRD diffraction pattern of BNNKT sintered ceramics at various temperatures. The pure perovskite phase was found in all ceramic samples. All the peaks of the solid solution system were indexed by pattern matching based on JCPDS data on BNT (36-0340) and $Bi_{0.5}K_{0.5}TiO_3$ (36-0339). At sintering temperature of 900 °C, splitting of a (003)/(021) peaks was detected in the 2θ range of 39-41° (Figure 59(b)) and the (202) peak is asymmetric in the range of 45-48° (Figure 59(c)). When sintering temperature is increased, the (003)/(021) peak begins to merge into a single (111) peak and the (202) peak starts to split into two peaks of (002)/(200). This characterizes indicated the coexistence of rhombohedral and tetragonal phases, which is consistent with the nature of the specimen with an MPB composition.

The SEM photographs of BNNKT-0.20/0.03 calcined powders at various temperatures are shown in Figure 60. It was found that the particle size exhibited spherical morphology. With increase in sintering temperature, the particle size trend to increase. The average particle size increased from 226 nm to 326 nm for BNNKT 0.20/0.03 withan increase of calcination temperature from 600°C to 850°C and is listed in Table 16.

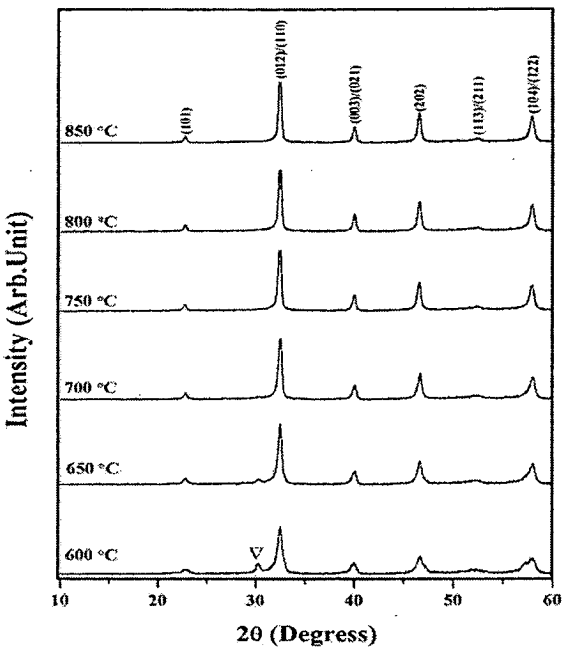

Figure 58 XRD patterns of BNNKT0.20/0.03 powders calcined at various temperatures for 2 h: (∇ $K_4Ti_3O_8$)

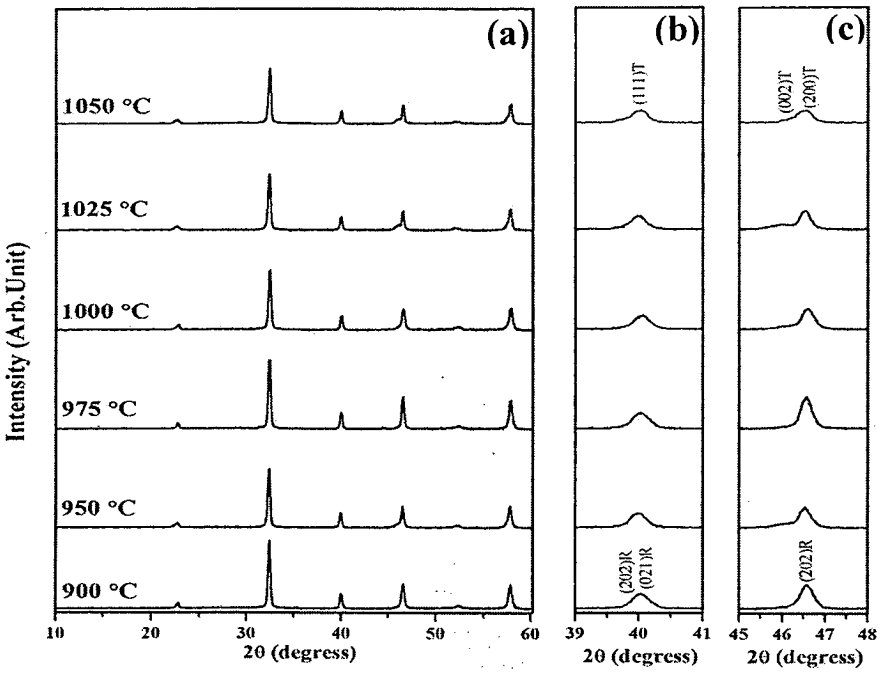

Figure 59 X-ray diffraction patterns of BNNKT-0.20/0.03 sintered ceramics in the 2θ range of (a) 10° to 60°, (b) 39° to 41° and (c) 45° to 48°

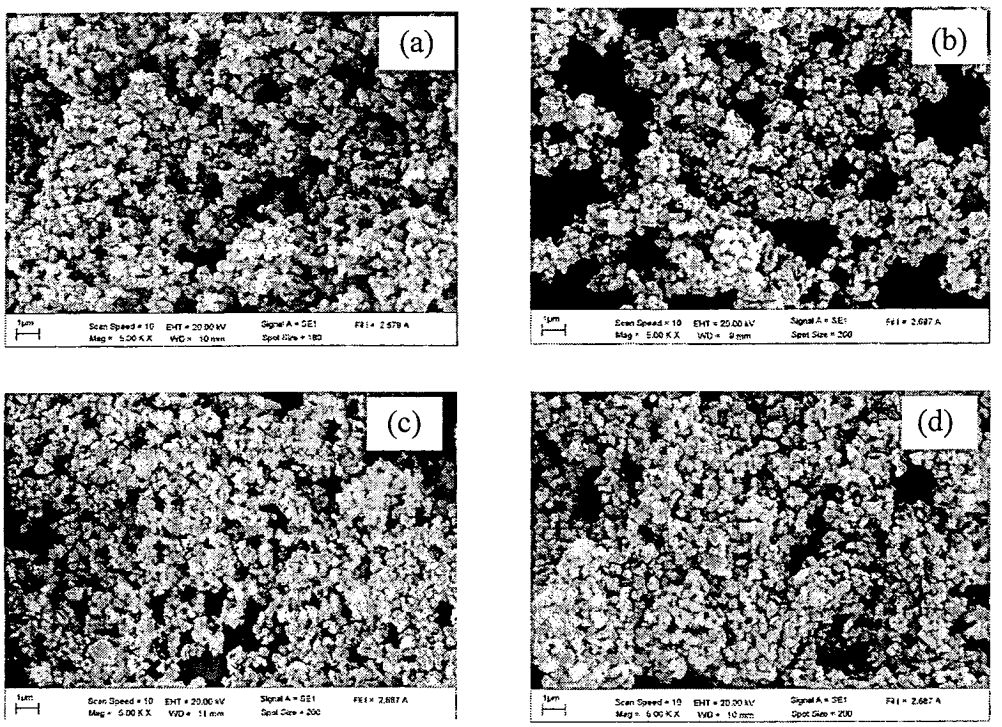

Figure 60 SEM images of BNNKT-0.20/0.03 calcined at (a) 600 °C, (b) 700 °C, (c) 800 °C and (d) 850 °C

Table 16 Percent perovskite phase, lattice parameter a, average particle size, average grain size, density and shrinkage of BNNKT

Calcination Temperature (°C)	Calcined powder			Sintering Temperature (°C)	Sintered ceramic			
	Perovskite phase (%)	Lattice parametera(Å)	Average particle size (nm)		Average grain Size (μm)	Measured density (g/cm^{-3})	Relative density (%)	Shrinkage (%)
600	79.5	3.8012±0.034	226±15.3	900	0.66	4.74	79.8	10.0
650	92.1	3.8166±0.066	249±10.4	950	0.70	5.21	87.8	11.3
700	95.2	3.8247±0.036	277±12.4	1000	0.82	5.37	90.5	13.9
750	100	3.8578±0.093	312±17.4	1025	1.13	5.64	95.5	16.4
800	100	3.8604±0.031	326±14.2	1050	1.29	5.41	91.2	15.0

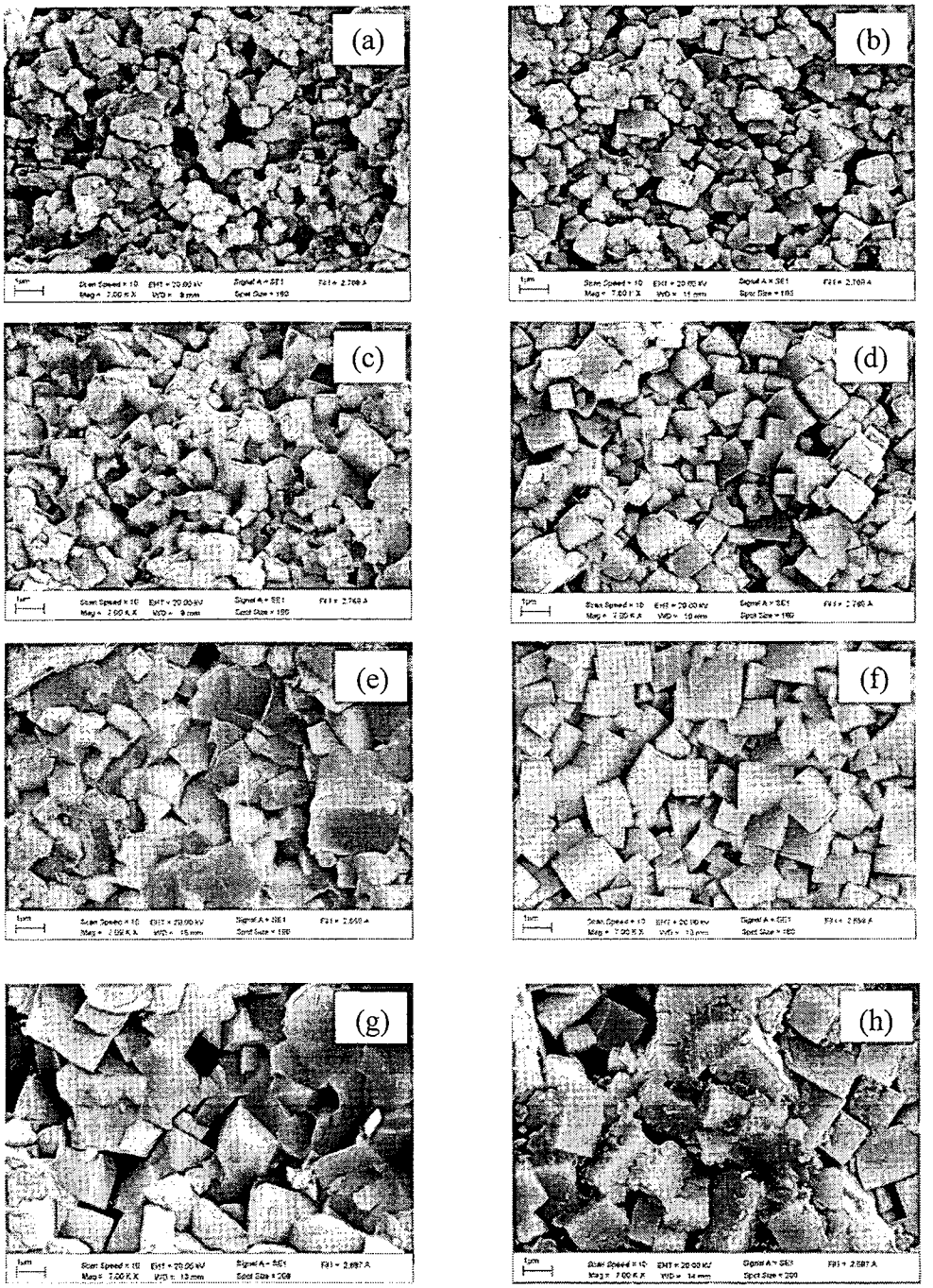

Figure 61 Cross-sectional and surface morphologies micrographs of the BNNKT-0.20/0.10 sintered ceramics at various temperatures: (a) and (b) sintered at 950 °C, (c) and (d) sintered at 1000 °C, (e) and (f) sintered at 1025 °C, (g) and (h) sintered at 1050 °C

Effect of x and y on crystal structure and microstructure of BNNKT ceramics

The optimum calcination and sintering temperature of all samples was found at 750 °C and 1025°C for 2 h, and it was then that the amounts of x and y on the crystal structure and microstructure were examined.The XRD patterns of BNNKT-x/0.03 ceramics at difference x content are shown in Figure 62. The XRD peaks indicated pure perovskite phase and no secondary phase can be found from the patterns in all samples. The diffraction peaks tend to shift to a lower angle with increasing x content, suggesting a contraction of the unit cell volume. This may be attributed to the radii of the A-and B-site ions of the unit cell in the system, which causes distortion of the unit cell. Generally, the rhombohedral structure is identified by (003)/(021) peaks splitting at 2θ range of and 39° to 41°and a single peak of (202) between 45° and 48°. While, the tetragonal structure is characterized by a single peak of (111) between 39 ° and 41° and (002)/(200) peaks splitting between 45° and 48°. At x =0.18, clearly observation of the (003)/(021) peaks spitting ~ 39°- 41°. In the 2θ range of and 45° to 48°, non-symmetry of (202) peak was observed. When x is increased, the (003)/(021) peak begins to merge into a single (111) peak and splitting of (202) peaks into (002) and (200) diffraction peaks can be observed. The XRD patterns of BNKKT-0.20/y ceramics are shown in Figure 62(a)-(c).At y=0,the XRD pattern show only (002)/(200) peaks splitting between 39° to 41° and a single peak of (111) between 45° to 48°.The peaks splitting begin to merge into a single peak with increasing y content. In the case of BNT-BKT binary system with $0.16 \leq x \leq 0.20$ studied by Yang et al[1], coexisting phases of rhombohedral and tetragonal was observed. The structure becomes more tetragonal with increased BKT content. Laoratanakul et al. [108] investigated the structure of$(1-x)Bi_{0.5}Na_{0.5}TiO_3$-$xK_{0.5}Na_{0.5}NbO_3$ with x=0-0.10. The structure identified the phase transition from rhombohedral and pseudo-cubic symmetry. Furthermore, the addition of KNN content decreased rhombohedral and the structure became more pseudo-cubic symmetry. The results of this work, in the composition of $0.18 \leq x \leq 0.28$, the structure exhibited co-existing phases between rhombohedral and tetragonal structures. For $0 \leq y \leq 0.07$, the structure exhibited co-exists phase rhombohedral to pseudo-cubic symmetry (Figure 63). The x (BKT)

content causes the increase in the tetragonal and the decrease in the rhombohedral phases. However, the increasing of y (KNN) content causes by the increase in the pseudo-cubic symmetry and decrease in the rhombohedral phase.

The SEM micrographs of BNNKT ceramics with x and y content are shown in Figure 64 and Figure 65, respectively. In general, the ceramics showed a quasi-cubic morphology and porous microstructure distribution with clear grain boundaries. The morphology of the ceramics is similar to result of BNNKT prepared by solid state reaction method [14].With increase of x and y content, the average grain size decreases from 1.42 μm to 1.02 μm and 1.25 μm to 0.70 μm, respectively.

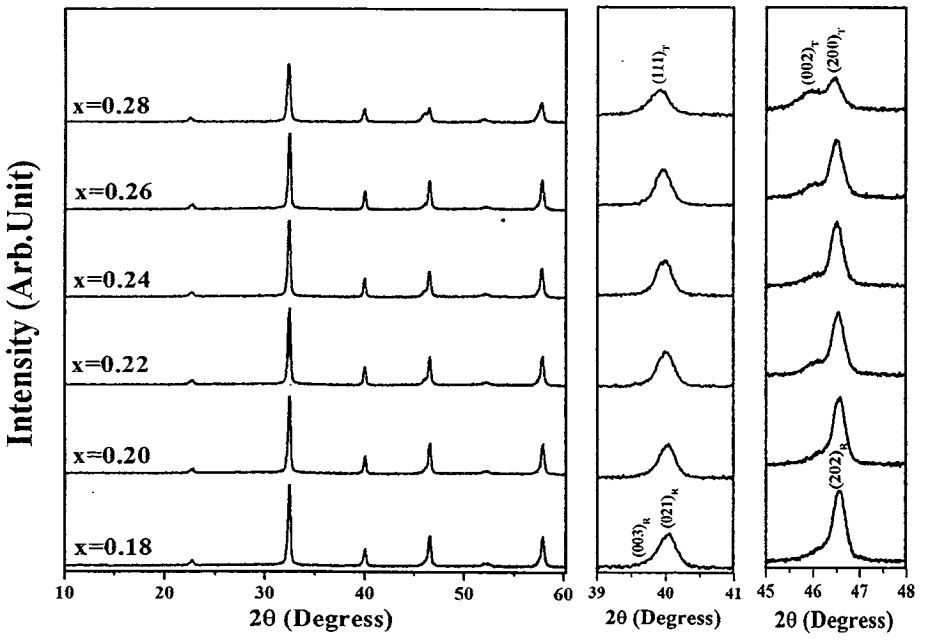

Figure 62 X-ray diffraction patterns of BNNKT-x/0.03 sintered ceramics in the 2θ range of (a) 10° to 60°, (b) 39° to 41° and (c) 45° to 48°

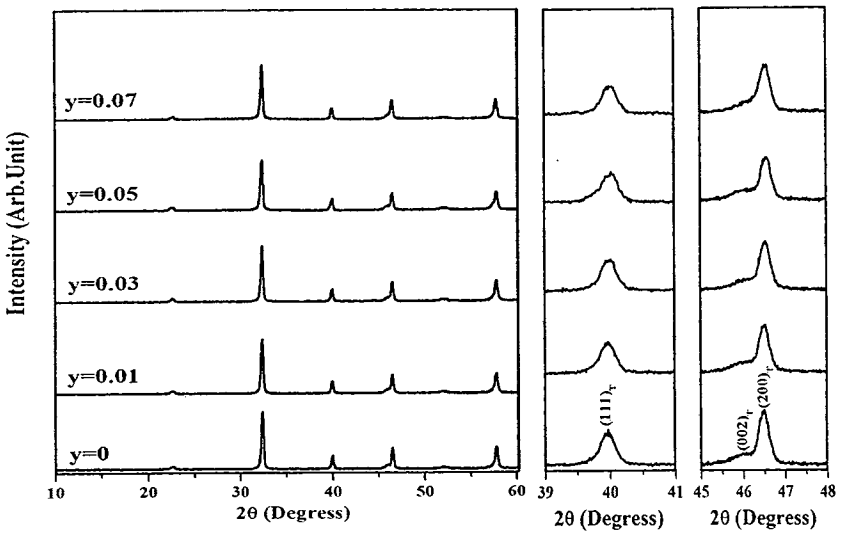

Figure 63 X-ray diffraction patterns of BNNKT-0.20/y sintered ceramics in the 2θ range of (a) 10° to 60°, (b) 39° to 41° and (c) 45° to 48°

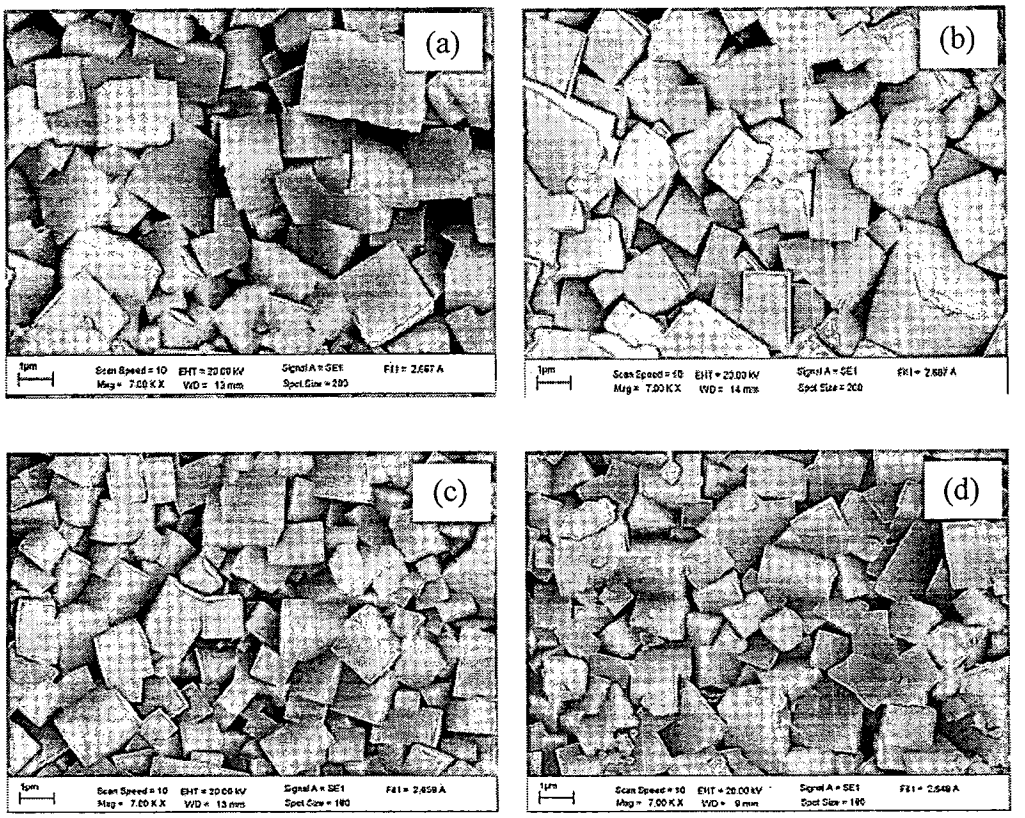

Figure 64 SEM images of BNNKT-x/0.03 sintered ceramics with (a) x= 0.18, (b) x=0.20, (c) x=0.22, (d) x=0.24, (e) x=0.26 and (f) x=0.28

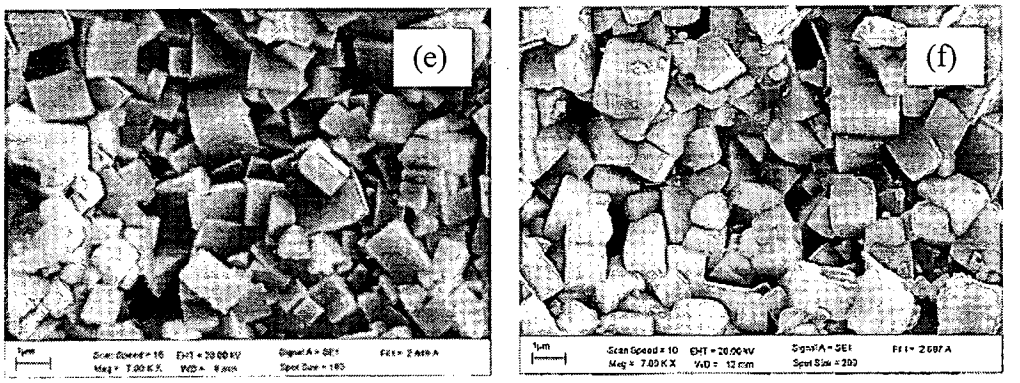

Figure 64 (cont.)

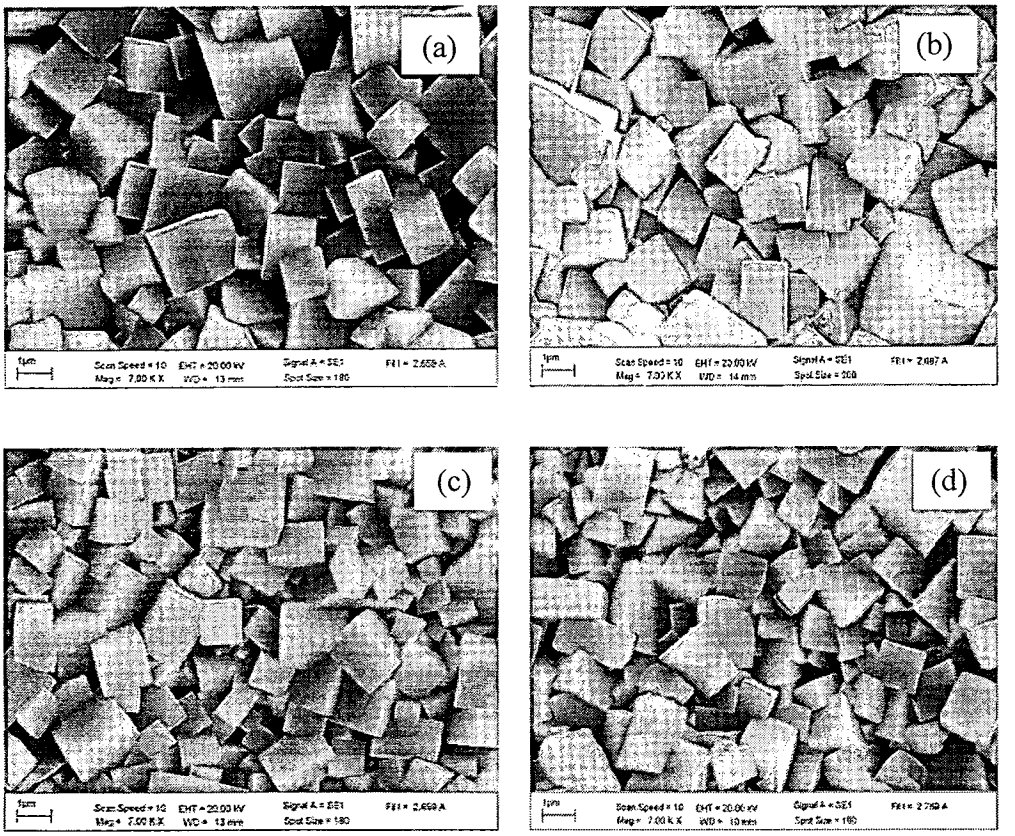

Figure 65 SEM images of BNNKT-0.20/y sintered ceramics with (a) y= 0, (b) y=0.01, (c) y=0.03, (d) y=0.05 and (e) y=0.07

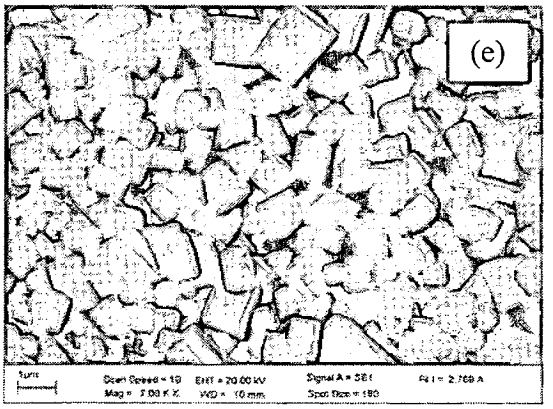

Figure 65 (cont.)

Effect of x and y on electrical properties of BNNKT ceramics

I. Dielectric properties of BNNKT ceramics

Figure 66 and Figure 67 show the temperature dependence of the dielectric constant (ε_r) of BNNKT-x/0.01 and BNNKT-0.20/y ceramics with x=0.18-0.28, respectively, as a function of temperature at 1 kHz. The dielectric curves of all samples look similar. There are two dielectric anomalies obvious humps (at T_d) and a broad dielectric constant peak (at T_m) within the measuring temperature range. T_d corresponds to the transition from a ferroelectric state to the anti-ferroelectric state. T_m corresponds to a transition from anti-ferroelectric to paraelectric state. This feature intrinsically comes from pure BNT, which was reported to have a diffuse structure phase transition from rhombohedral ferroelectric to tetragonal anti-ferroelectric at ~200 °C and a Curie phase transition from anti- ferroelectric to paraelectrical phases at ~320 °C [109]. (1-x-y)BNT-xBKT-yKNNceramics may show similar phase transition behavior. However, the phase transition was changed with addition x (BKT) and y (KNN) contents. When x content increased from 0.18 to 0.24, T_d decreased from 119 - 96 °C, and then increasedwith increase inx content. For composition of y content, T_d decreased from 114 - 84 °C with increasing x up to y=0.03 (see Table 1). At y > 0.03, T_d increased from 84 to 108 °C. The maximum dielectric initially increases with addition of BKT up to x = 0.20 where maximum value of ~ 5,200 is observed. With a further increase of x content above 0.20, value of maximum dielectric constant is observed to decrease. For composition of y content,

the maximum dielectric constant decreased from 5,818 to 4,034 with increasing y up to y=0.05 and then increased the value of 5,031 at y = 0.07.

The temperature dependence of the dielectric constant (ε_r) of BNNKT-x/0.01 and BNNKT-0.20/y ceramics which were measured at different frequency are shown in Figure 66 and Figure 67, respectively. The ε_r show pronounced dependence on frequency. With increased frequency, ε_r for all ceramics decrease. Moreover, both T_d and T_m exhibit obvious dependence on the frequency. With increasing frequency, T_d moves to higher temperature regions and T_m moves to lower temperature regions. The tanδ reaches the maximum value around T_d and no second dielectric loss peak occurs. The reason may be that tanδincreases sharply above T_m due to the high conductivity of the ceramics at high temperature. However, when the temperature is higher or lower than T_d and T_m, the ε_r does not show evident upshift with increasing frequency. The broad ε_r peaks and the character of the temperature dependence of ε_r shows typical relaxation characteristic. Relaxor phase transition has been observed in many ABO_3-type perovskites and bismuth layer-structure compounds, such as $(1-x)Bi_{1/2}Na_{1/2}TiO_3$-$xBaTiO_3$[110], $Bi_{1/2}Na_{1/2}TiO_3$–$Bi_{1/2}$ $K_{1/2}TiO_3$–$SrTiO_3$ [99], $Bi_{1/2}Na_{1/2}TiO_3$–$Bi_{1/2}$ $K_{1/2}TiO_3$ [61,62], of which either the A-sites or B-sites are occupied by at least two cations. For the BNNKT ceramics, Na^+, Bi^+, Nb^+ and K^+ are randomly distributed in the 12-fold coordination sites, so the observed relaxor behavior is reasonably attributed to the disordering of the A-site cations and the compositional fluctuation.

The dielectric behavior of complex ferroelectrics with diffuse phase transition can be explained by the modified Curie–Weiss law according to the formula (15),where γ and Care assumed to be constant, γ value is between 1 and 2. When γ =1, the materials with this type phase transition can be called normal ferroelectrics; when 1 <γ< 2, the materials with this type phase transition are called relaxor ferroelectrics; whereas γ=2, the materials correspond to a so-called "complete" diffuse phase.

$$\frac{1}{\varepsilon} - \frac{1}{\varepsilon_m} = C(T - T_m)^{\gamma} \qquad (15)$$

Figure 68 shows the plot of $Ln(1/\varepsilon-1/\varepsilon_m)$ as a function of $Ln(T-T_m)$ for all ceramics samples at 1 kHz. The diffuseness exponent (γ) of ceramics are between 1.817 and 1.939 for composition of x (Figure 68(a)) and between 1.766 and 1.999 for composition of y (Figure 68(b)), indicating that the BNNKT-x/y solid solutions are diffuse phase transition behavior.These results imply an elevation of the relaxor feature and transition from normal ferroelectric to relaxor ferroelectrics.

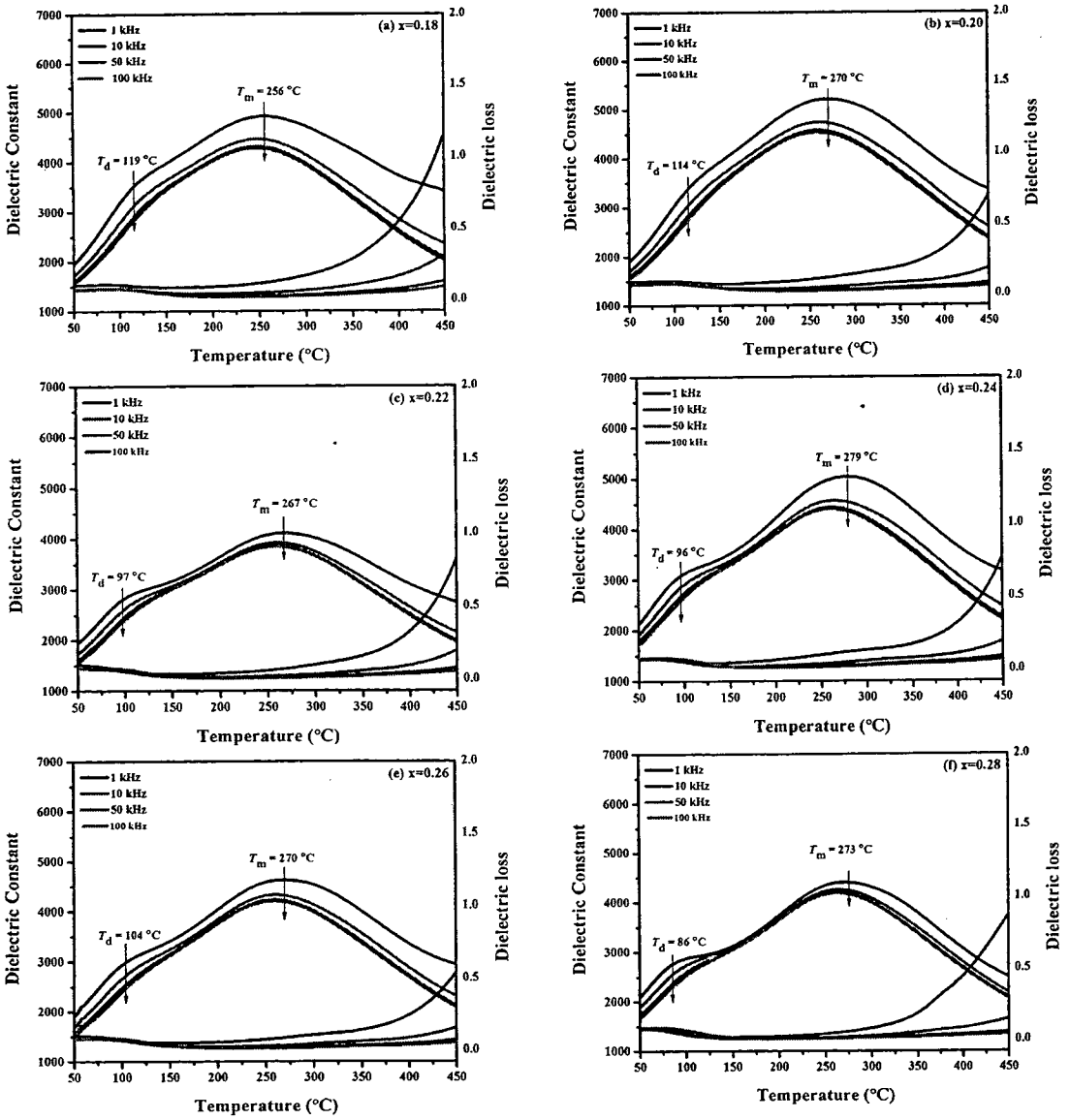

Figure 66 Temperature dependence of dielectric properties in the BNNKT system: (a) BNNKT-0.18/0.03, (b) BNNKT-0.20/0.03, (c) BNNKT-0.22/0.03, (d) BNNKT-0.24/0.03, (e) BNNKT-0.26/0.03 and BNNKT-0.28/0.03

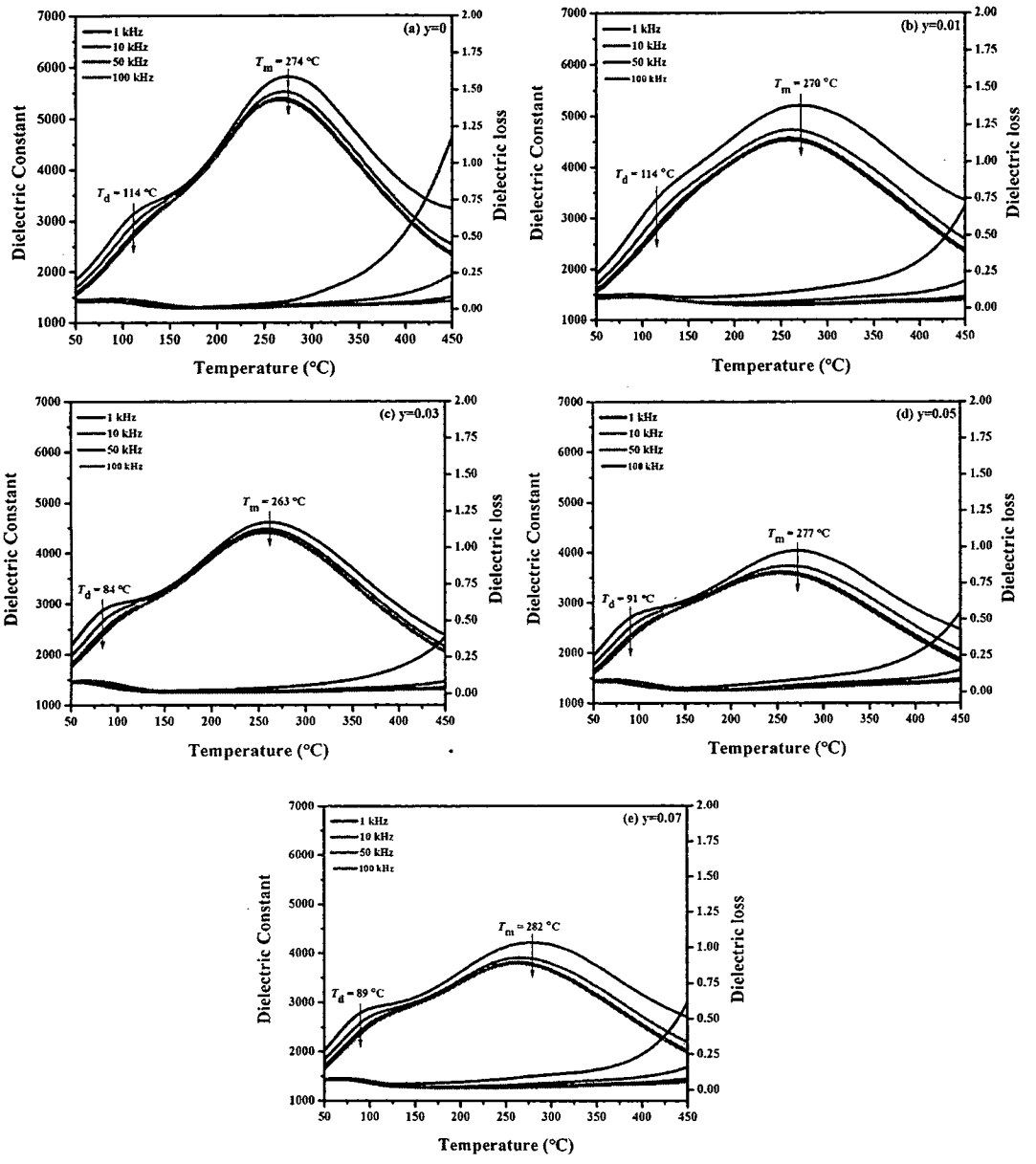

Figure 67 Temperature dependence of dielectric properties in the BNNKT system: (a) BNNKT-0.20/0, (b) BNNKT-0.20/0.01, (c) BNNKT-0.20/0.03, (d) BNNKT-0.20/0.05 and (e) BNNKT-0.20/0.07

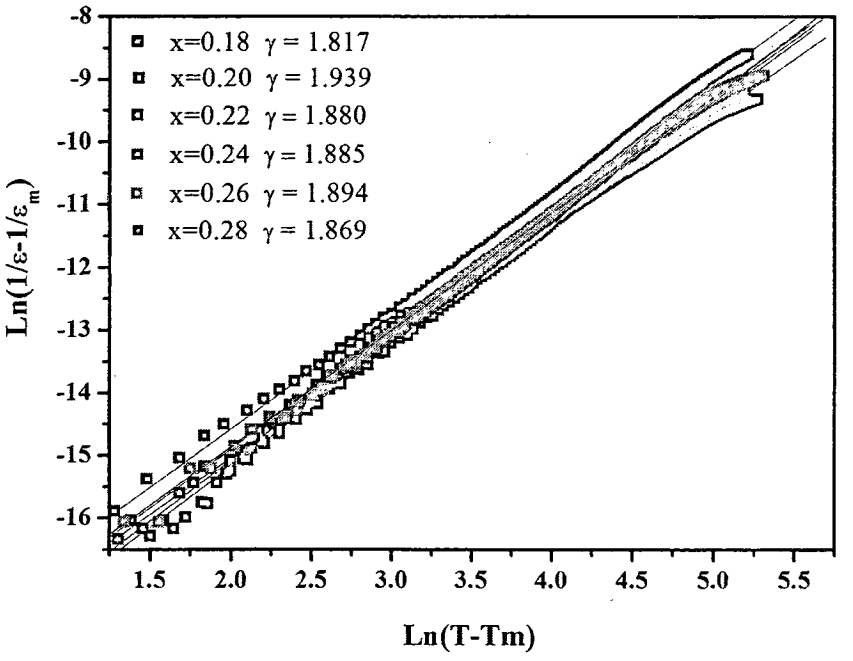

(a)

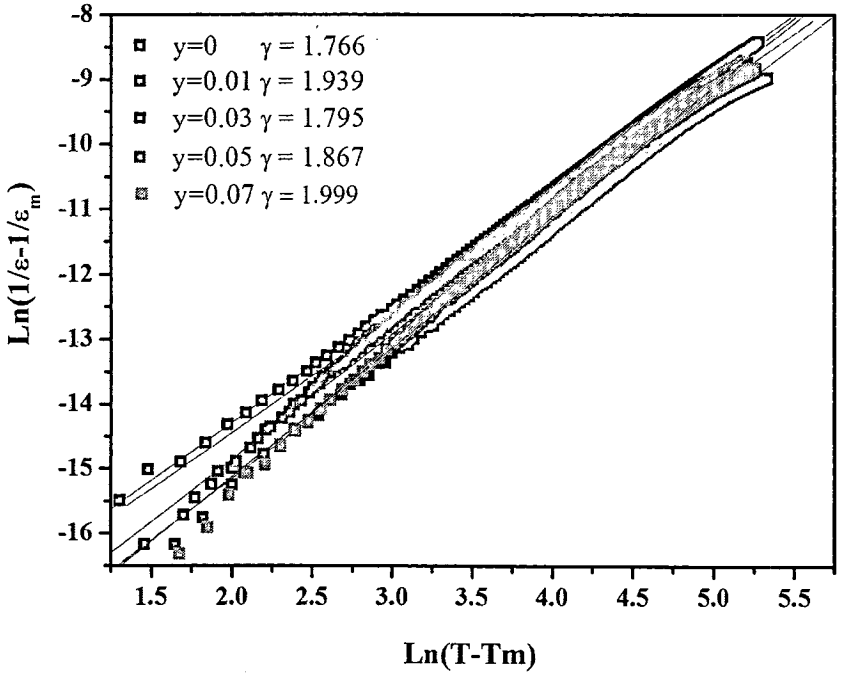

(b)

Figure 68 Logarithm of $(1/\varepsilon-1/\varepsilon_m)$ against logarithm of $(T-T_m)$ for the BNNKT system measured at 1 kHz
(a) BNNKT-x/0.01 and (b) BNNKT-0.20/y

II. Ferroelectric properties of BNNKT ceramics

The P-E hysteresis loop of BNNKT-x/0.03 and BNNKT-0.20/y ceramics measured at 0.1 Hz is shown in Figure 70 (a) and 70 (b), respectively. At x=0.18, the polarization hysteresis loops exhibited a well saturated typical ferroelectric behavior with remnant polarization P_r~34.2 $\mu C/cm^2$ and coercive field E_c~ 21.9 kV/cm, which better than the previous work which have been reported [106, 109]. When there was increased inx content (0.20, 0.22, and 0.24), the P_r and E_c both decrease rapidly and P-E hysteresis loops turn to be pinched and like-antiferroelectric behavior. When x> 0.24, the polarization hysteresis loop has becomes very weak and displays paraelectric phase behavior. The same trend was found in the sample of y content, as seen in Figure 70(b). The change of P-E loops indicates that the long-range ferroelectric order of the sample was disturbed and turned to the PNRs with increased of x and y contents.

III. Piezoelectric properties of BNNKT ceramics

The S-E hysteresis loops of BNNKT-x/0.03 and BNKLT-0.20/y ceramics were measured at 0.1 Hz and presented in Figure 71(a) and Figure 71(b), respectively. When y = 0, the S-E loops exhibited a butterfly shaped which is typical for materials with ferroelectric order. The negative strain (S_{neg}) ~0.08%, maximum strain (S_{max}) ~0.13 % and corresponded to a high-field effective d_{33}* of 266 pm/V (determined from the unipolar strain response under 0.1 Hz) were observed. As the concentration of y further increased, the S-E loops changed to become more parabolic and the negative strain generally decreased. These parabolic strain characteristics are similar to the electrostrictive behavior in relaxor ferroelectrics. The largest S_{max} of 0.25% corresponded to a high-field effective d_{33}* of 509 pm/V, which was found in the composition of y=0.01, as seen the ternary diagram of S_{max} and d_{33}* in Figure 69. The d_{33}* values are nearly twice those previously reported for BNT-BKT (291 pm/V) or BNT-BT (240 pm/V). The same trend was found in the sample of x content, as seen in Figure 71(b).

The piezoelectric coefficients of BNNKT-x/0.03 and BNNKLT-0.20/y ceramics are illustrated in Table 17. The piezoelectric coefficients (d_{33}) decreased slightly from 167-103 pC/N with increasing of x content. When y=0, the piezoelectric

coefficients d_{33} are 145 pC/N. With increasing content of y, d_{33} reached the maximum values of 168 pC/N at y=0.01, and then dropped in value.

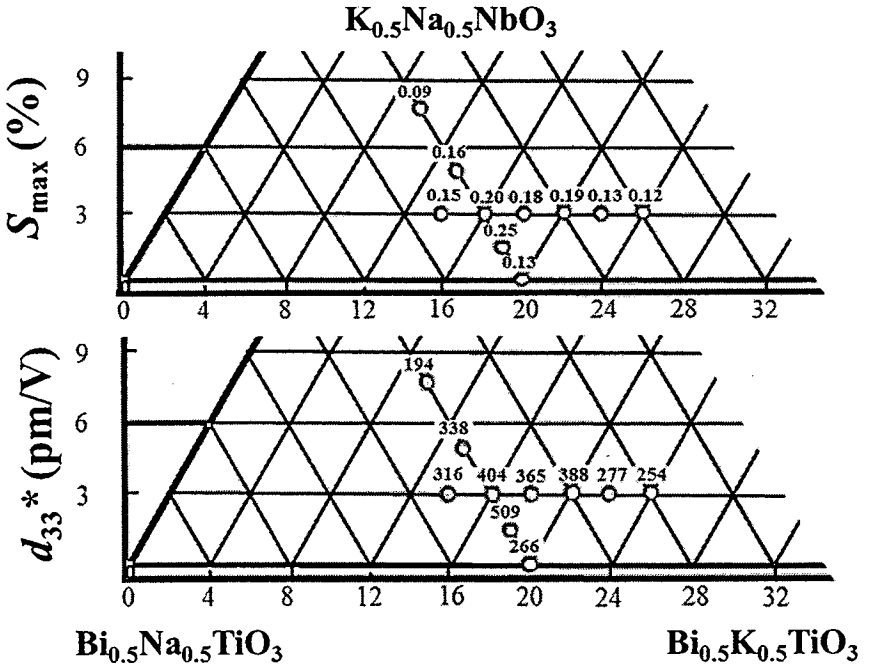

Figure 69 S_{max} (%) and d_{33}* (pm/V) values plotted on the BNNKT phase diagram

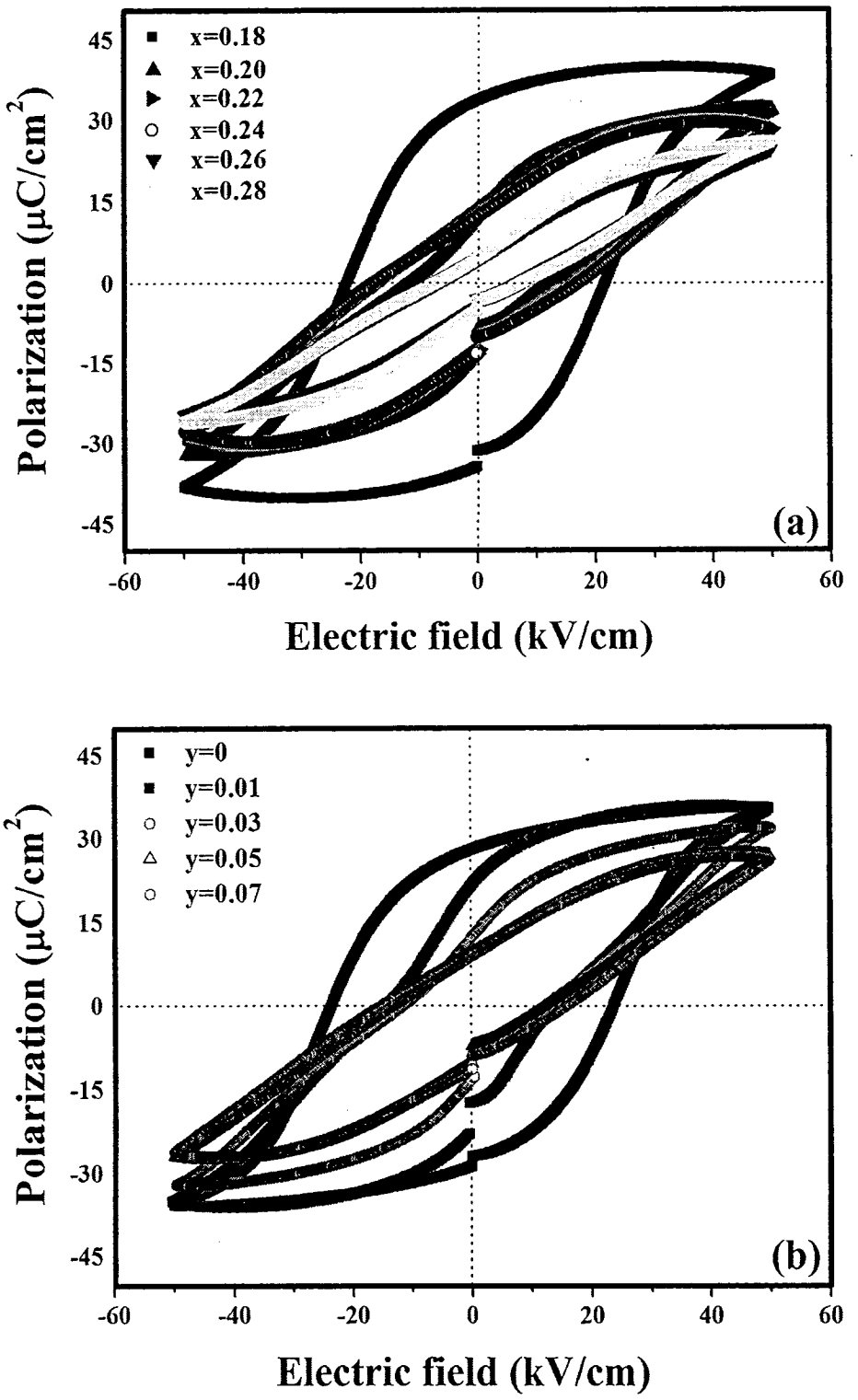

Figure 70 P-E hysteresis loop of (a) BNKKT-x/0.10 and (b) BNKKT-0.20/y ceramics measured at 0.1 Hz

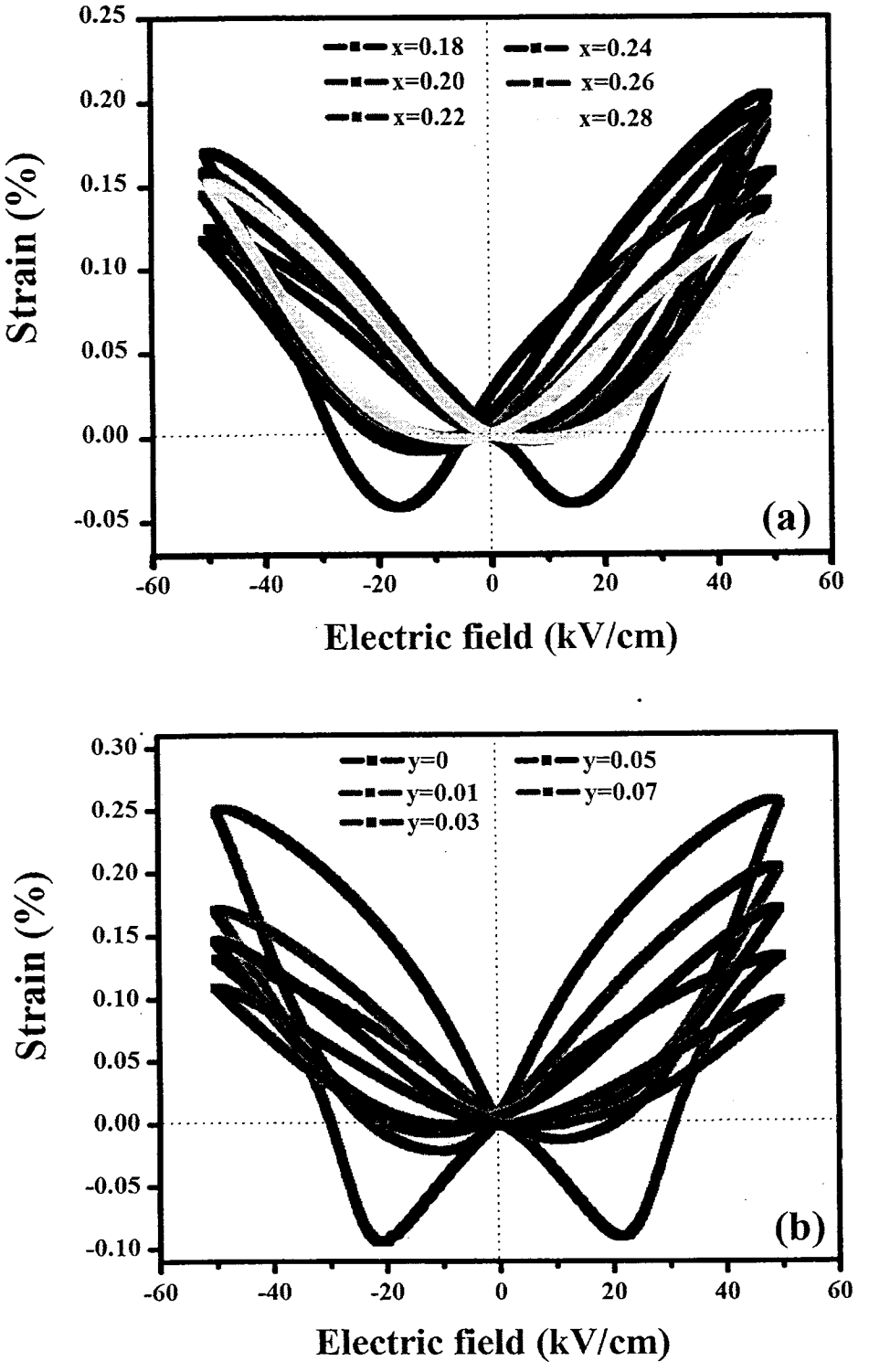

Figure 71 Strain loop of (a) BNNKT-x/0.10 and (b) BNNKT-0.20/y ceramics measured at 0.1 Hz

Table 17 Average grain size, T_d, T_m, P_r, E_c, ε_r, S_{Max}, S_{Neg}, S_{Max}/E_{Max} and d_{33} of BNNKT-x/y ceramic

Compositions	Average grain size (μm)	T_d (°C)	T_m (°C)	ε_r	γ	P_r (μC/cm^2)	E_c (kV/cm)	Strain (%)		S_{Max}/E_{Max} (pm/V)	d_{33} (pC/N)
								S_{Max}	S_{Neg}		
x=0.18	1.42	119	256	4,927	1.817	34.2	21.9	0.15	0.04	316	167
x=0.20	1.23	114	270	5,200	1.939	12.5	12.0	0.20	0.005	404	164
x=0.22	1.05	97	267	4,109	1.880	13.4	16.7	0.18	0.003	365	157
x=0.24	1.04	96	279	5,030	1.885	13.3	17.8	0.19	0.003	388	114
x=0.26	1.02	104	270	4,627	1.894	4.4	7.2	0.13	0.001	277	109
x=0.28	1.02	86	273	4,397	1.869	4.4	7.2	0.12	0.001	254	103
y=0	1.25	114	274	5,818	1.766	28.0	23.7	0.13	0.08	266	145
y=0.01	1.23	114	270	5,200	1.939	22.0	14.3	0.25	0.01	509	168
y=0.03	1.14	84	263	4,614	1.795	12.5	12.0	0.20	0.005	404	164
y=0.05	1.03	91	277	4,034	1.867	9.8	12.9	0.16	0.001	338	120
y=0.07	0.70	108	282	5,031	1.999	9.8	15.7	0.09	0.001	194	84

Conclusion

BNNKT powders and ceramics were successfully prepared by combustion technique with calcination and sintering of 750 °C and 1025 °C for 2 h. The calcination and sintering parameters have direct effect on phase formation, grain size, densification microstructure and dielectric properties of ceramics samples. The BNNKT powder showed the rhombohedral structure. The BNNKT sintered ceramics indicated the coexistence of rhombohedral and tetragonal phases, which is consistent with the nature of the specimen with an MPB composition. The result shows that the increase of sintering temperature helped the growth of grain size. The density and shrinkage increased with increasing sintering temperatures from 900°C to 1025°C, and decreased after further sintering at a higher temperature (1050°C).BNNKT powders and ceramics can be successfully synthesized by the combustion technique at a lower calcination and sintering temperatures than those prepared by the solid-state reaction method.

The variations of x and y contents directly affect the crystal structure, microstructure, density and electrical properties on BNNKT-x/y ceramics. The structure identified the phase transition from rhombohedral and pseudo-cubic symmetry. The addition of KNN content decreased rhombohedral phase and the structure became more pseudo-cubic.With increase of x and y content, the average grain size decreases. The ε_r show pronounced dependence on frequency. With increased frequency, ε_r for all ceramics decrease. The BNNKT-x/y solid solutions exhibited diffuse phase transition behavior. The change in P-E loops indicated that the long-range ferroelectric order of the sample was disturbed and turned to the PNRs with increase of x and y contents. The polarization hysteresis loop transformed from well saturated typical ferroelectric to pinched and then to relaxor state with increase in x and y contents. The largest S_{max} of 0.25% corresponding to a high-field effective d_{33}* of 509 pm/V was found in the composition withy=0.01.